Global Journal of Science Frontier Research
Physics and Space Science
Volume 13 Issue 4 Version 1.0 Year 2013
Type : Double Blind Peer Reviewed International Research Journal
Publisher: Global Journals Inc. (USA)
Online ISSN: 2249-4626 & Print ISSN: 0975-5896

A Review of Higher Order Statistics and Spectra in Communication Systems

By M. Sanaullah
Purdue University Calumet USA

Abstract - There are many statistical tools to extract information from random signals. They predominantly use first and second order statistics. However, in the presence of nonlinearity in systems, many signals cannot be analyzed adequately by second order statistical methods. For this reason, higher order statistical methods have been developed. These methods are very useful in problems where non-Gaussian, non-minimum phase, phase coupling or nonlinear behavior and robustness to additive noise are important. Detection and classification using higher order statistical and spectral techniques have been proposed for use in communication and pattern recognition. They have the potential to elicit better performance from sensors, sensor networks and channels with applications in coding, filtering and detection techniques. This paper provides an introduction to higher order spectra and reviews a number of these techniques.

Keywords : higher order spectra, high order statistics, interference, bispectrum, invariant, entropy, fading.

GJSFR-A Classification : FOR Code: 010401

A REVIEW OF HIGHER ORDER STATISTICS AND SPECTRA IN COMMUNICATION SYSTEMS

Strictly as per the compliance and regulations of :

© 2013. M. Sanaullah. This is a research/review paper, distributed under the terms of the Creative Commons Attribution-Noncommercial 3.0 Unported License http://creativecommons.org/licenses/by-nc/3.0/), permitting all non commercial use, distribution, and reproduction in any medium, provided the original work is properly cited.

A Review of Higher Order Statistics and Spectra in Communication Systems

M. Sanaullah

Abstract - There are many statistical tools to extract information from random signals. They predominantly use first and second order statistics. However, in the presence of nonlinearity in systems, many signals cannot be analyzed adequately by second order statistical methods. For this reason, higher order statistical methods have been developed. These methods are very useful in problems where non-Gaussian, non-minimum phase, phase coupling or nonlinear behavior and robustness to additive noise are important. Detection and classification using higher order statistical and spectral techniques have been proposed for use in communication and pattern recognition. They have the potential to elicit better performance from sensors, sensor networks and channels with applications in coding, filtering and detection techniques. This paper provides an introduction to higher order spectra and reviews a number of these techniques.

Keywords : higher order spectra, high order statistics, interference, bispectrum, invariant, entropy, fading.

I. Introduction

Higher order statistics and spectra (HOS) play an important role in digital signal processing. They are extensions of the better known concepts of correlation (in time or space) and power spectra. Just as the power spectrum is the Fourier spectral representation of the autocorrelation function which is a second order moment of the probability density function, higher order spectra are higher order Fourier spectral representations of third and higher order correlations or moments.

Higher order spectra were originally introduced as spectral representations of cumulants or moments of ergodic random processes. They were used in the identification of nonlinear systems and non-Gaussian random processes and phase coupling in wave-wave interactions. Papers by Brillinger and Rosenblatt [1, 2] laid the theoretical foundations of the area and the paper by Hasselman et al [3] in 1963 that studied bispectra of ocean waves was one of the earliest applications. Signal processing theory and applications of HOS grew with the excellent review paper in 1987 by Nikias and Raghuveer [4] and the books on HOS in 1993 by Nikias and Petropulu [5] and in 1995 by Boashash, Powers and Zoubir [6].

Author : M. Sanaullah is now with the Department of Electrical & Computer Engineering, Purdue University Calumet, IN 46323, USA.
E-mail : hi.sanam@yahoo.com

Over the years, HOS have been applied in many areas in a stochastic framework and their application has been extended to deterministic signals. Although there are similarities in the forms of analytical expressions for both the stochastic and the deterministic frameworks, there are important differences that must be understood in order to apply HOS effectively to practical problems. Many of the later contributions to application of HOS to practical problems are now scattered in various journals and proceedings of conferences. Techniques for detection and classification using HOS have been proposed and many application contributions have been published in journals that are outside the IEEE/IEE research collection.

Higher order spectra have potential for application in continuing and recent research efforts in the fields of communication and pattern recognition. A communications engineer doing research on Multiple Input Multiple Output (MIMO) wireless communications could benefit from an understanding of the capabilities of HOS in order to make better use of phase information, adapt to non-Gaussian noise or adapt to non-linear channel characteristics. Similarly, a biomedical engineer can use HOS to derive features from EEG or ECG signals which represent output data from systems where the input is not known. Polyspectra play a key role in detecting and characterizing the type of nonlinearity in a system from its output data. Several signal processing methods for the detection and characterization of nonlinearities in time series using higher order spectra have been proposed. Some of the early developments are found in Rao and Gabr [14] and Nikias and Petropulu [5].

The paper is organized as follows. Section II provides definitions and properties. Section III provides a tutorial on the use of HOS. Section IV reviews contributions relevant to the chosen application areas. Research trends and potential for future applications are discussed in Section V followed by a conclusion in Section VI.

II. Higher Order Statistics: Definitions and Properties

Random variables $x \in \Re^N$ (scalars or vectors) have probability densities $p_X(x)$. If a probability density is Gaussian,

© 2013 Global Journals Inc. (US)

$$p_X(x) = [\,2\pi]^{-N/2}[\det(C)]^{1/2} exp\left\{-\frac{(x-m_x)^T C^{-1}(x-m_x)}{2}\right\} \quad (1)$$

it is completely characterized by the mean value, m, (a first order statistic) and the covariance , C, (a second order statistic). In an estimate of the mean, values of a random vector are considered independently.

$$m_X = \iiint_{=\infty}^{\infty} x\, p_X(x)\; dx \quad (2)$$

In an estimate of the covariance, values of the random vector (or random vectors in the case of joint statistics) are considered in pairs.

$$\sigma_X^2 = \; diag\left[\iiint_{-\infty}^{\infty} (x-m_x)^T (x-m_x)\, p_X(x)\, dx\right] \quad (3)$$

If the probability density function of the random variable is continuous and well behaved enough for a Fourier transform to exist in the form of a Fourier-Stieltjes integral, its Fourier transform, called the characteristic function, can be represented in a power series expansion. Such an expansion has the mean and the covariance in its first two terms.

$$\Phi(f) = \sum_{k=0}^{n} \frac{1}{k!} m_X^k (jf)^k + o_n(f)$$

$$= 1 + jfm_1 - \frac{f^2}{2!} m_2 \ldots\ldots + \frac{(jf)^k}{k!} m_k + \cdots \quad (4)$$

where the remainder function $o_n(f)$ is such that $o_n(f)/f^n$ goes to zero in the limit as f approaches zero.

Subsequent terms are expected values of higher (than second) order products of samples of the random variable – referred to as the higher order moments of the distribution. It is often convenient to remove the mean value or first moment and expand the probability density function about the mean. This results in central moments of the distribution which have the useful property of being invariant to a shift of the origin.

It is not necessary that moments of all orders exist and are finite. Some moments can be infinite. The distribution is not always uniquely determined by the moments either even when moments of all order exist. The log-normal distribution is an example. However, in general, the higher order moments serve to determine the distribution more accurately.

Higher order moments for a Gaussian probability density are constant but not zero. If the logarithm of the characteristic function is expanded instead, the higher order terms represent expected values of combinations known as cumulants, and these are zero for a Gaussian density.

$$\Psi(f) = \sum_{k=1}^{n} \frac{1}{k!} c_x(k)(jf)^k + o_n(f) \quad (5)$$

where $c_x(k) = (-j)^k \left.\frac{d^k \Psi(f)}{df^k}\right|_{f=0}$ $for\ k = 1,2,3,$ and $\Psi(f) = \ln\{\Phi(f)\}$

The remainder function, $o_n(f)$, is such that $o_n(f)/f^n$ goes to zero in the limit as f approaches zero. If the probability density is non-Gaussian it is not completely represented by its mean and covariance. The higher order cumulants are then non-zero.

Random processes $\underline{x}(t): t \to \Re$ are random functions of some independent variable such as time. Each realization of the process is one of an ensemble of possible functions. If a vector of values, at different time delays from a reference variable time, is considered, there is an ensemble of realizations of random vectors.

$$x(t) = \bar{x}(t, t+\tau_1, t+\tau_2, \ldots\ldots, t+\tau_{n-1}) \in \Re^n \quad (6)$$

For such a process, the joint density of the random vector represents the ensemble statistics and it can in general be a function of time t. For an n-th order stationary process, the joint density is independent of time. However, it still depends on the time lags or separations between the random variables. Again assuming that the joint probability density function is well behaved and a Fourier transform exists, the characteristic function can be expressed as

$$\Phi(f) = \int_{-\infty}^{+\infty} \exp(j2\pi f x)\, p_X(x)\; dx \quad (7)$$

From the above formulation it can also be noted that the moments of this joint probability density are also the correlations in time of the underlying random process. The second moment is the auto-correlation of the process. A Fourier transform of the auto-correlation is the power spectrum of the random process. Higher order correlations will give rise to higher order spectral representations for the process. Thus higher order statistics of the joint density function of random variables separated by time lags are related to higher order spectra for the underlying random process.

If the random process is zero mean, the first moments of the density function will be zero. If the random process is white, random variables at different delays will be uncorrelated and the second moments will be described by a diagonal covariance matrix of variances. If the random process is Gaussian, the joint density function can be described by the means and covariance matrix alone, and higher order moments are functions of these parameters. Higher order moments take on non-zero values because on some sub-manifolds of the n-th order lag space, they can degenerate to products of lower order moments. For example, a fourth order moment can degenerate to a product of two variances if two of the four lags are identical and so are the other two. In this case, there are

© 2013 Global Journals Inc. (US)

only two random variables rather than four. Such degeneracy can occur whenever the set of n random variables can be split into two or more statistically independent groups. Higher order cumulants account for these sub-manifolds and are zero for Gaussian processes. Cumulants other than the first are also invariant to a shift of the origin like the central moments.

$$\Psi(f) = \Psi_1(a_1 f) + \Psi_2(a_2 f) + \cdots + \Psi_n(a_n f) \quad (8)$$

Cumulants are not directly ascertained through summation or integration but they are related to moments and can be found using these relationships. When working with real-world signals in a random process framework, probability density functions are in most cases not known in closed form. Moments must be estimated from realizations of the signal. It is then important to understand time and ensemble statistics of the process and assumptions about stationarity and ergodicity.

If scalar random variables are considered, the expected value over the ensemble is the ensemble mean of the process. There is a corresponding expectation in time, the time mean of the process. For an ergodic process, the ensemble statistics and the time statistics are assumed to be identical. If the product of two values of the process, separated by a time lag is considered, the autocorrelation function of the process is obtained. For a second order ergodic process, the time autocorrelation and ensemble autocorrelation are equal. If the autocorrelation, $R_{xx}(\tau)$ is well behaved enough for a Fourier transform to exist, its Fourier transform yields the power spectral density of the process.

$$P_{xx}(f) = \int_{-\infty}^{\infty} R_{xx}(\tau) e^{-j2\pi f\tau}\, d\tau \quad (9)$$

If the two values come from two different random processes, a cross-correlation is obtained and its Fourier transform represents the cross-spectral density of the two processes.

$$P_{xy}(f) = \int_{-\infty}^{\infty} R_{xy}(\tau) e^{-j2\pi f\tau}\, d\tau \quad (10)$$

The autocorrelation and the cross-correlation and the corresponding spectra form the basis of powerful second order approaches to signal detection, estimation and tracking such as matched filtering, Wiener filtering and Kalman filtering. For a stationary and ergodic process, these concepts were extended to products of three and more values separated by lags, by Shiryaev [7] and laid on firm mathematical foundations by Brillinger [8] and Rosenblatt [1, 2]. They lead to the definition of higher order cumulant functions and corresponding higher order spectra.

For auto-correlation and auto-spectra we can omit the subscripts assuming that these are implied The Fourier transform of the third order cumulant function is referred to as the bispectrum and it is a complex-valued function of two frequencies.

$$B(f_1, f_2) = \int_{-\infty}^{\infty} R(\tau_1, \tau_2) e^{-j2\pi(f_1\tau_1 + f_2\tau_2)} d\tau_1 d\tau_2 \quad (11)$$

The Fourier transform of the fourth order cumulant function is referred to as the trispectrum. It may be noted that these Fourier spectra exist only when the cumulant functions are well behaved – they decay with increasing lag and are absolutely integrable, for example. Conditions for existence can be relaxed carefully and the definitions and estimation procedures can be extended to include cyclostationary and harmonic random processes. The power spectral density $P(f)$ of a random process $x(t)$ can be represented using

$$P(f)df = E[dX(f)dX^*(f)] \quad (12)$$

This makes use of the Cramer spectral representation

$$x(t) = \int_{-\infty}^{\infty} \exp[j2\pi ft] dX(f) \quad (13)$$

Similarly the bispectrum $B(f_1, f_2)$ can be represented using

$$E[dX(f_1)dX(f_2)dX^*(f_3)] = \begin{cases} B(f_1, f_2)df_1 df_2 & f_1 + f_2 = f_3 \\ 0 & \text{otherwise} \end{cases} \quad (14)$$

It is estimated using the averaged biperiodogram. E represents expectation over an ensemble of realizations of the process. The periodogram and the biperiodogram are computed using numerical samples over a time windowed realization of the process and the Fast Fourier transform. Averaging is performed with several realizations.

The theoretical foundations have been extended and conditions for existence relaxed in a number of ways. Discrete-time processes are not integrable but the use of Z transforms, discrete Fourier transforms and absolute summability allows definition of higher order cumulants and spectra for them. Deterministic functions do not have ensemble statistics or ensemble probability density functions. However, they have time statistics and it has been shown that

$$B(f_1, f_2) = X(f_1)X(f_2)X^*(f_1 + f_2)$$
$$= \int_{-\infty}^{\infty} \tilde{R}(\tau_1, \tau_2) \exp[-j2\pi(f_1\tau_1 + f_2\tau_2)] d\tau_1 d\tau_2 \quad (15)$$

where* represents the complex conjugate and $\tilde{R}(\tau_1, \tau_2)$ is the third order correlation in time (represented by $\mathcal{E}$) of the deterministic function.

© 2013 Global Journals Inc. (US)

$$\tilde{R}(\tau_1,\tau_2) = \mathcal{E}[x(t)x(t+\tau_1)x(t+\tau_2)]$$
$$= \int_{-\infty}^{\infty} x(t)x(t+\tau_1)x(t+\tau_2)dt \qquad (16)$$

The third order correlation, or third order moment, is a function of two lag variables and the bispectrum is a function of two frequency variables. The above equations show that it is possible to estimate the bispectrum in two ways: either computing the third moment function and then taking its Fourier transform, or computing the Fourier transform of the function and using triple products of Fourier coefficients. For continuous-time deterministic signals, integrability of the moment and the existence of the Fourier transform are necessary for validity. For discrete-time signals or for computation via numerical methods based on sampling, summability of the moment and existence of the discrete-time Fourier transform are necessary for validity. The corresponding equations in discrete time are

$$B(f_1,f_2) = X(f_1)X(f_2)X^*(f_1+f_2)$$
$$= \sum_{n_1=-\infty}^{\infty}\sum_{n_2=-\infty}^{\infty}\tilde{R}(n_1,n_2)\exp[-j2\pi(f_1n_1+f_2n_2)] \qquad (17)$$

where $B(f_1,f_2)$ is the bispectrum of x(n), $\tilde{R}(n_1,n_2)$ is the third order correlation and *X(f)* is the Fourier transform of x(n) which are shown in equation (9) and (10). In general, $B(f_1,f_2)$ is complex and a sufficient condition for its existence is that $\tilde{R}(n_1,n_2)$ is absolutely summable.

$$\tilde{R}(n_1,n_2) = \mathcal{E}[x(n)x(n+n_1)x(n+n_2)]$$
$$= \sum_{n=-\infty}^{\infty} x(n)x(n+n_1)x(n+n_2) \qquad (18)$$

$$X(f) = \sum_{n=-\infty}^{\infty} x(n)\exp[-j2\pi fn] \qquad (19)$$

The sampling interval in the above equations is assumed to be unit, and when frequencies are normalized by the sampling frequency, the bispectrum, $B(f_1,f_2)$ is periodic in f_1 and f_2 with period 2π radians/sec or 1 cycle/sec. For a real-valued input, the spectrum is conjugate symmetric and only positive frequencies up to one-half the sampling frequency are unique in spectral values. Therefore, frequencies are often normalized by one half of the sampling frequency (or Nyquist frequency). Further, the bispectrum is symmetric in the two frequencies and knowledge of the auto-bispectrum in the triangular region $f_2 \geq 0, f_1 \geq f_2, f_1+f_2 \leq 1$ (see Fig. 1) is enough for its complete description, where frequencies are normalized by the Nyquist frequency and the input is real-valued.

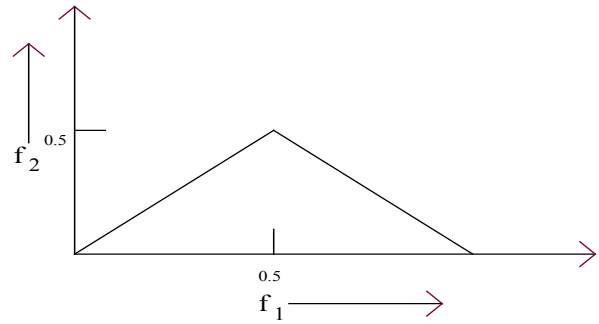

Figure 1 : Triangular bounded by $f_2 = 0, f_1 = f_2, f_1 + f_2 = 1$. Values of $B(f_1,f_2)$ on this triangle for a real-valued and band-limited random process determine its values everywhere in the $(f_1 - f_2)$ plane

For a full description of the non-redundant regions of computation of various higher order spectra, the reader is referred to [5, 9]. The discrete-time versions may be further extended to discrete versions that are also sampled in the frequency domain. This is required to be able to compute spectra numerically. It may be noted that frequency sampling inherently makes the sequence periodic in time. Equivalently, computing the spectra using finite length sequences yields the discrete Fourier transform (DFT) which is a sampled version of the discrete-time Fourier transform (DTFT).

$$X(k) = \sum_{n=0}^{N-1} x(n)\exp[-j2\pi kn] \qquad (20)$$

For deterministic signals, the assumption of periodicity outside the window of observation leads to side effects such as spectral leakage. Equation (20) is used with time samples x(n) in the frequency domain approach to obtain Fourier coefficients and their products are used in estimation via the first part of equation (15) or (17), in the frequency domain approach. Equation (20) is used with moments $\tilde{R}(n_1,n_2)$ in the direct approach. If the observation window [0, N-1] is long enough for the moment function to have decayed sufficiently, the frequency sampling should not cause significant error.

Higher-order spectra are thus multidimensional Fourier transforms of higher-order statistical parameters [10]. For stochastic processes, a frequency domain approach is beset with some difficulty because a Fourier transform does not strictly speaking exist for a stationary random process. However, spectral representations as in equations (13) and (14) can be employed with the use of expected values as done in stochastic calculus [10]. Discrete spectral representations imply conversion to cyclostationary processes but if the moments of interest decay to nearly zero within the observation window estimation of their spectra via expectations of products of frequency domain samples as in a discrete version of

© 2013 Global Journals Inc. (US)

equation (14) will be valid. In order to apply the frequency domain approach to estimation, each realization of a random process is windowed in time and sampled and equation (20) is used to computer Fourier coefficients. Averaging over an ensemble as in equation (14) reduces the estimation variance, taking the estimate closer to the true value.

The trispectrum is defined in terms of the fourth order cumulant by the discrete Fourier transform (DFT):

$$T(f_1,f_2,f_3) = X(f_1)X(f_2)X(f_3)X^*(f_1+f_2+f_3)$$
$$= \sum_{n_1=-\infty}^{\infty}\sum_{n_2=-\infty}^{\infty}\sum_{n_3=-\infty}^{\infty} c_4^x(n_1,n_2,n_3)\exp[-j2\pi(f_1n_1+f_2n_2+f_3n_3)] \quad (21)$$

where $c_4^x(n_1,n_2,n_3)$ is the fourth-order cumulant sequence, similar to third-order cumulant given by equation (18) for bispectrum. The expectation operation in the tri-periodogram is omitted above, when the signal is deterministic. Symmetry properties and non-redundant region of computation of the trispectrum are discussed in [9].

If a distribution is symmetric, then its third-order cumulant equals zero; hence, for such a process we must use fourth-order cumulants. For example, Laplace, Uniform, Gaussian and Bernoulli-Gaussian distributions are symmetric, whereas Exponential, Rayleigh and k-distributions are non-symmetric. Some processes have distributions with extremely small third-order cumulants and much larger fourth-order cumulants; hence, for such processes also we would also use the fourth cumulant or the trispectrum. In cubically phase coupled harmonic random processes also, the third order cumulants equal zero whereas fourth-order cumulants are non-zero.

If $\{x(k)\}$ is, $k = 0, \pm1, \pm2, \pm3, \ldots$ is a real stationary discrete-time signal and its moments up to order n exist, then

$$m_n^x(\tau_1,\tau_2,\ldots,\tau_{n-1}) \triangleq E\{x(k)x(k+\tau_1)x(k+\tau_2)\ldots x(k+\tau_{n-1}\} \quad (22)$$

represents the nth-order moment function of the signal, which depends only on the time differences $\tau_1,\tau_2,\ldots,\tau_{n-1}, \tau_i = 0, \pm1, \pm2, \ldots.$ for all i. The 2nd –order moment function, $m_2^x(\tau_1)$, is the autocorrelation whereas $m_3^x(\tau_1,\tau_2)$ and $m_4^x(\tau_1,\tau_2,\tau_3)$, the 3rd and 4th order moments, respectively, are the third and fourth order (auto) correlations of the signal. The nth-order cumulant function of a non-Gaussian stationary random signal $x(k)$ can be written as (for n=3, 4 only):

$$c_n^x(\tau_1,\tau_2,\ldots,\tau_{n-1}) = m_n^x(\tau_1,\tau_2,\ldots,\tau_{n-1}) - m_n^G(\tau_1,\tau_2,\ldots,\tau_{n-1}) \quad (23)$$

where $m_n^x(\tau_1,\ldots,\tau_{n-1})$ is the nth-order moment function of $x(k)$ and $m_n^G(\tau_1,\tau_2,\ldots,\tau_{n-1})$ is the nth-order moment function of an equivalent Gaussian signal that has the same mean value and autocorrelation sequence as $x(k)$.Clearly, if $x(k)$ is Gaussian, $m_n^x(\tau_1,\tau_2,\ldots,\tau_{n-1}) = m_n^G(\tau_1,\tau_2,\ldots,\tau_{n-1})$ and thus $c_n^x(\tau_1,\tau_2,\ldots,\tau_{n-1}) = 0$. Note, however, that although equation (14) is only true for orders n=3 and 4, $c_n^x(\tau_1,\tau_2,\ldots,\tau_{n-1}) = 0$ for all n if $X(k)$ is Gaussian.

The relation between moments and cumulants are shown by the following equations which exist for orders n=1,2,3,4 for the sequence of $\{x(k)\}$.

1st –order cumulants:

$$c_1^x = m_1^x = E \quad (24)$$

2nd –order cumulants:

$$c_2^x(\tau_1) = m_2^x(\tau_1) - (m_1^x)^2$$
$$= m_2^x(-\tau_1) - (m_1^x)^2 = c_2^x(-\tau_1) \quad (25)$$

where $m_2^x(-\tau_1)$ is the autocorrelation sequence. Thus, we see that the 2nd order cumulant sequence is the covariance while the 2nd order moment sequence is the autocorrelation.

3rd –order cumulants:

$$c_3^x(\tau_1,\tau_2) = m_3^x(\tau_1,\tau_2)$$
$$-m_1^x[m_2^x(\tau_1)+m_2^x(\tau_2)+m_2^x(\tau_1-\tau_2)] + 2(m_1^x)^3 \quad (26)$$

where $m_3^x(\tau_1,\tau_2)$ is the third-order moment sequence. This follows if we combine equation (22) and (23).

4th –order cumulants:

Combining equation (22) and (23), we get

$$c_4^x(\tau_1,\tau_2,\tau_3) = m_4^x(\tau_1,\tau_2,\tau_3)$$
$$-m_2^x(\tau_1).m_2^x(\tau_3-\tau_2) - m_2^x(\tau_2).m_2^x(\tau_3-\tau_1)$$
$$- m_2^x(\tau_3).m_2^x(\tau_2-\tau_1)$$
$$- m_1^x[m_3^x(\tau_2-\tau_1,\tau_3-\tau_1) + m_3^x(\tau_2,\tau_3) + m_3^x(\tau_3,\tau_1)$$
$$+ m_3^x(\tau_1,\tau_2)]$$
$$+ (m_2^x)^2[m_1^x(\tau_1)+m_2^x(\tau_2)+m_2^x(\tau_3)+m_2^x(\tau_3-\tau_1)$$
$$+ m_2^x(\tau_3-\tau_2)+m_2^x(\tau_2-\tau_1)]$$
$$- 6(m_1^x)^4 \quad (27)$$

If the signal $\{x(k)\}$ is zero mean $m_1^x = 0$, it follows from equation (25) and (26) that the second- and third-order cumulants are identical to the second- and third-order moments, respectively; however, to generate the fourth-order cumulants, we need knowledge of the fourth-order and second-order moments in equation (27), i.e.,

$$c_4^x(\tau_1,\tau_2,\tau_3) = m_4^x(\tau_1,\tau_2,\tau_3) - m_2^x(\tau_1).m_2^x(\tau_3-\tau_2)$$
$$- m_2^x(\tau_2).m_2^x(\tau_3-\tau_1)$$
$$- m_2^x(\tau_3).m_2^x(\tau_2-\tau_1) \quad (28)$$

© 2013 Global Journals Inc. (US)

The use of cumulants rather than moments has a number of advantages as pointed out by J. Mendel [11].

1. If $\lambda_i, i = 1,2, \ldots, k$ are constants and $x_i, i = 1,2, \ldots, k$ are random variables, then $cum(\lambda_i x_i, \ldots \lambda_k x_k) = \prod_{i=1}^{k} \lambda_i \, cum\,(x_1, \ldots x_k)$
2. Cumulants are symmetric in their arguments, i.e., $cum(x_1, \ldots \ldots, x_k) = cum(x_{i_1}, \ldots \ldots, x_{i_k})$ where $(i_1, \ldots \ldots, i_k)$ is a permutation of $(1, \ldots \ldots, k)$
3. Cumulants are additive in their arguments, i.e., $cum(x_0 + y_0, z_1, \ldots, z_k) = cum(x_0, z_1, \ldots, z_k) + cum(y_0, z_1, \ldots, z_k)$ This means that cumulants of sums equals sums of cumulants (hence, the name "cumulant").
4. If α is a constant, then $cum(\alpha + x_1, x_2, \ldots \ldots, x_k) = cum(x_1, x_2, \ldots \ldots, x_k)$
5. If the random variables $\{x_i\}$ are independent of the random variables $\{y_i\}, i = 1,2, \ldots \ldots, k$ then $cum(x_1 + y_1, \ldots, x_k + y_k) = cum(x_1, \ldots, x_k) + cum(y_1, \ldots, y_k)$
6. If a subset of the k random variables $\{x_i\}$ is independent of the rest, then $cum(x_i, \ldots, x_k) = 0$

Cumulants of an independent, identically distributed random sequence are delta functions, if $w(t)$ is an i.i.d. process, then $C_{k,w}(\pi_1, \pi_2, \ldots \ldots, \pi_{k-1}) = \gamma_{k,w}\delta(\pi_1)\delta(\pi_2) \ldots \delta(\pi_{k-1})$, where $\gamma_{k,w}$ is the kth –order cumulant of the stationary random sequence $w(n)$.

This makes the higher-order statistics more robust to additive measurement noise than second order correlation, even if that noise is colored. In essence, cumulants can draw non-Gaussian signals out of Gaussian noise; thereby boosting their signal-to-noise ratios [11].

At a glance, Figure 2 illustrates the various higher-order spectra for a given discrete-time signal. Although higher-order statistics and spectra of a signal can be defined in terms of moments and cumulants, moments and moment spectra are very useful in the analysis of deterministic signals (transient and periodic) whereas cumulant and cumulant spectra are more useful in the analysis of stochastic signals. The two spectra are identical up for order three (the bispectrum). Unlike the power spectrum which is real-valued, higher order spectra can be complex valued and have both magnitude and phase, in general. The phase of the bispectrum is referred to as biphase and that of the trispectrum as the triphase.

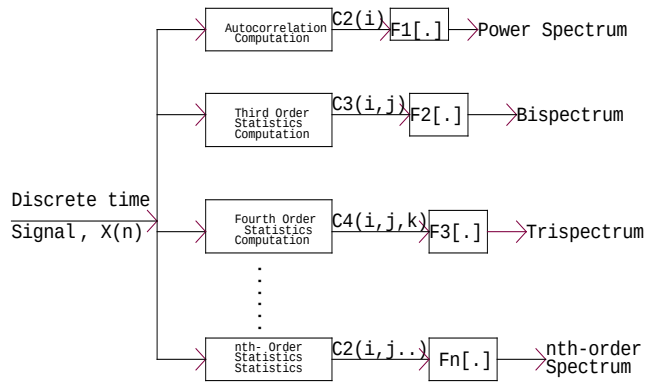

Figure 2 : The various higher order spectra for a deterministic signal. F [.] denotes n-dimensional Fourier Transform

Higher order spectra are also functions of two or more component frequencies unlike the power spectrum which is a function of a single frequency. Although numerically computed estimates of higher order spectra may have non-zero values, they may or may not be statistically significant. Statistical significance depends on the number of degrees of freedom in the estimate. Of particular interest in the analysis of phase coupling between Fourier components is the value of the magnitude of the higher order spectrum independent of the powers at the component frequencies. This can be achieved by normalizing the magnitude with powers at the component frequencies. Since non-linear interactions result in the generation of phase-coupled power at sum and difference frequencies, the normalized spectra are also useful in detection and characterization of non-linearity in systems. A normalized higher-order spectrum or nth-order coherency index is a function that combines the cumulant spectrum of order n with the power spectrum (n=2) of a signal. For a discrete- time signal, the 3rd – and 4th –order coherence are respectively defined by

$$B_{x(bico\,herence\,)}(f_1, f_2) = \frac{B_x(f_1, f_2)}{\sqrt{P_x(f_1)P_x(f_2)P_x(f_1 + f_2)}} \quad (29)$$

$$T_{x(trico\,herence\,)} = \frac{T_x(f_1, f_2, f_3)}{\sqrt{P_x(f_1)P_x(f_2)P_x(f_3)P_x(f_1 + f_2 + f_3)}} \quad (30)$$

These functions are very useful in the detection and characterization of nonlinearities in time series and in discriminating linear processes from nonlinear ones. A signal is said to be a linear non-Gaussian process of order n if the magnitude of the nth-order coherence, $|(P)_n^x(f_1, f_2, \ldots, f_{n-1})|$, is constant over all frequencies; otherwise, the signal is said to be a non-linear process[13]. They are also useful in detecting phase coupling between Fourier components.

© 2013 Global Journals Inc. (US)

III. Tutorial on Higher Order Statistics

A random signal, $x(n)$ is completely characterized by its Autocorrelation Function (ACF) only if it originates from a random process with Gaussian characteristics. In non-Gaussian processes, the higher order moments carry information that cannot be found in the ACF. Such signals can be found for example in speech, radar, sonar, bio-medicine, seismic data processing, plasma physics and optics. General relations for arbitrary stationary random data passing through arbitrary linear systems have been studied quite extensively for many years, but similar extensive general results are not available for arbitrary stationary random data passing through arbitrary nonlinear systems. Instead, each type of nonlinearity has been investigated as a special case. The extra information provided by HOS leads to better estimates of parameters and sheds light on non-linearity in the source of the signal. In addition, cross-polyspectra may be used for nonlinear system identification from observations of input and output data. In this section we represent some brief examples to the readers of how higher order spectral have been applied to the following tutorial topic.

a) Quadratic/Cubic Phase Coupling

Quadratic phase coupling are situations where because of interaction between two harmonic components of a process there is contribution to the power at their sum and/or difference frequencies. A special case is when have two components with one being at twice the frequency of the other. For example, suppose the signal

$$x(n) = A_1 \sin(\lambda_1 n + \theta_1) + A_2 \sin(\lambda_2 n + \theta_2)$$

is passed through the following simple nonlinear system:

$$z(n) = x(n) + cx^2(n) \tag{31}$$

where c is a non-zero constant. The signal $z(n)$ contains sinusoidal terms in (λ_1, θ_1), (λ_2, θ_2), $(2\lambda_1, 2\theta_1)$, $(2\lambda_2, 2\theta_2)$, $(\lambda_1 + \lambda_2, \theta_1 + \theta_2)$ and $(\lambda_1 - \lambda_2, \theta_1 - \theta_2)$. Such phenomena, which give to rise to all of these phase relations, are known as quadratic phase coupling [12] and arise from the quadratic (square law) non-linearity.

In particular applications, such as EEG data analysis, oceanography and plasma physics, it is necessary to find out if peaks at harmonically related positions in the power spectrum are in fact phase-coupled. Since the power spectrum suppresses all phase relations it cannot provide an answer. The bispectrum, on the other hand, is capable of detecting and characterizing quadratic phase coupling. Consider the harmonic random process

$$x(n) = \sum_{i=1}^{6} \sin(\lambda_i n + \theta_i) \tag{32}$$

where $\lambda_1 > \lambda_2 > 0$, $\lambda_4 > \lambda_5 > 0$, $\lambda_3 = \lambda_1 + \lambda_2$, $\lambda_6 = \lambda_4 + \lambda_5$, $\theta_1, \theta_2, \ldots \ldots \theta_5$ are all independent, uniformly distributed r.v.s over $(0, 2\pi)$ and $\theta_6 = \theta_4 + \theta_5$. In equation (32) while $(\lambda_1, \lambda_2, \lambda_3)$ and $(\lambda_4, \lambda_5, \lambda_6)$ are at harmonically related positions, only the component at λ_6 is a result of phase coupling between those at λ_4 and λ_5 while the one at λ_3 is an independent harmonic component. The power spectrum of the process consists of impulses at $\lambda_i; i = 1,2, \ldots ,6$ as illustrated in Figure 3.

Looking at the power spectrum one cannot say if the harmonically related components are, in fact, involved in quadratic phase-coupling relationships. The third-moment sequence $m_3^x(\tau_1, \tau_2)$ of $x(n)$ can be easily obtained as

$$\begin{aligned} m_3^x(\tau_1, \tau_2) = \frac{1}{4}\{&\sin(\lambda_5\tau_1 + \lambda_4\tau_2) + \sin(\lambda_6\tau_1 + \lambda_4\tau_2) \\ &+ \sin(\lambda_4\tau_1 + \lambda_5\tau_2) + \sin(\lambda_6\tau_1 - \lambda_5\tau_2) \\ &+ \sin(\lambda_4\tau_1 - \lambda_6\tau_2) \\ &+ \sin(\lambda_5\tau_1 - \lambda_6\tau_2)\} \end{aligned} \tag{33}$$

It is important to observe that in equation (33) only the phase coupled components appear.

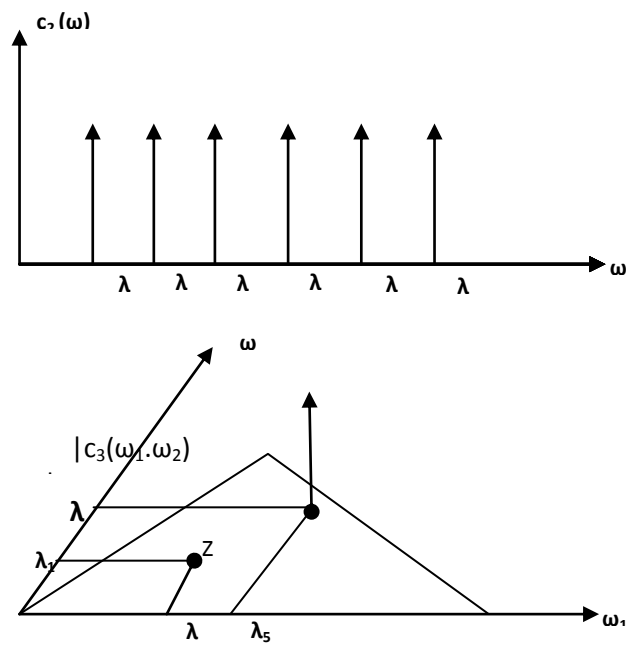

Figure 3 : Quadratic phase coupling (a) Power spectrum of the process described by equation (31) and (b) its magnitude bispectrum

Consequently, the bispectrum evaluated in the triangular region of Figure 3 shows an impulse only at (λ_4, λ_5) indicating that only this pair is phase coupled. In the total absence of phase coupling the third moment sequence and the bispectrum are both zero. Thus the fact that only phase coupled components contributes to the third moment sequence of a process is what makes the bispectrum a very useful diagnostic tool for non linear wave interactions.

© 2013 Global Journals Inc. (US)

In the example above, the third moment and the bispectrum were computed analytically using knowledge of the probability density functions of the phases. In practice, sampled data are available from the process and the question must be answered by numerical computation and hypothesis testing. If we simulate 100 realizations of this process, each of length 512 samples, sampled at 6 times the highest frequency component, with components of equal and unit amplitude at frequencies $\lambda_1 = 10, \lambda_2 = 20, \lambda_3 = 30, \lambda_4 = 40, \lambda_5 = 50, \lambda_6 = 90,$ such that each phase is uniform random in $[0,2\pi)$ and the phase relationship $\theta_6 = \theta_4 + \theta_5$ holds in each realization, a power spectral density of the process computed using an averaged periodogram estimate with no windowing would be as shown in Figure 4

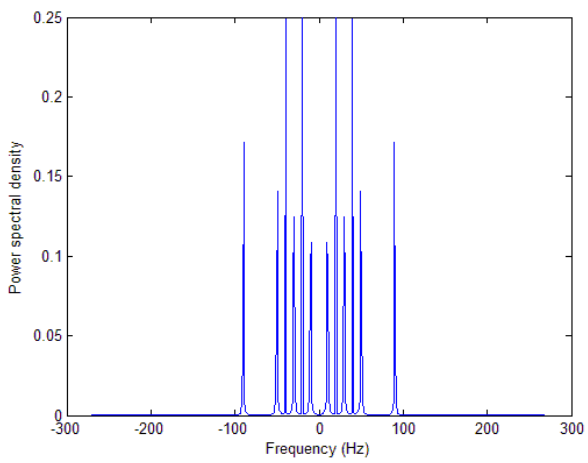

Figure 4 : Power spectral density of the process defined in equation 21, when estimated using an averaged periodogram estimate from 100 realizations

It can be observed that estimates of the power spectral density are not all equal because of the variance of the estimate and spectral leakage owing to the finite length discrete Fourier transform. The power spectrum does not reveal any phase information and does not distinguish between the peaks at the different frequencies. It does not tell us whether the peak at 90 Hz is related to those at 40 Hz and 50 Hz, or whether the peaks at 10 Hz, 20 Hz and 30 Hz are phase coupled. If we estimate the bispectrum of this process using an averaged biperiodogram method, its magnitude (Figure 5) shows a prominent peak at (50 Hz, 40 Hz) as expected. There is no such peak at (20 Hz, 10 Hz) because these components were not phase coupled to the component at 30 Hz. However, smaller peaks are also observed at other frequency combinations, again arising from the fact that statistical zero is not numerically zero and there is spectral leakage around the true peaks. The other peaks are much smaller in magnitude than the peak at (50 Hz, 40 Hz) which is where the bispectrum is statistically significantly different from zero.

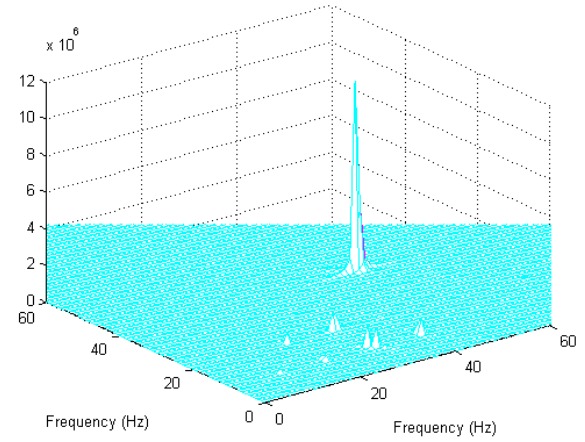

Figure 5 : Magnitude bispectrum for the process in equation (21) estimated from 100 simulated realizations

If we compute the bicoherence, normalizing as done by Kim and Powers, bicoherence values are found to be between 0 and 1. For 100 realizations averaged, the bicoherence is statistically significantly different from zero only when the value is above 6/200 or 0.03. A plot of the bicoherence is shown in Figure 6.

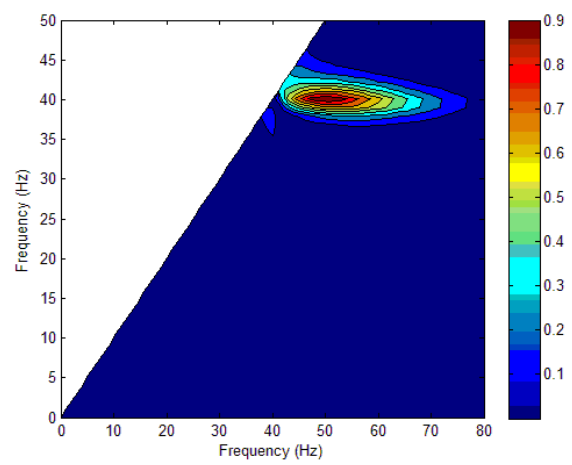

Figure 6 : Bicoherence for the processing in equation (21) estimated from 100 realizations. Only the bifrequency region of interest is shown here. A statistically significant non-zero value occurs at (50 Hz, 40 Hz) as expected

Only the region of frequencies that are of interest is shown here – not the entire triangular non-redundant region, the rest of which has statistically zero bicoherence. It can be observed here that the only value above 0.03 is at (50 Hz, 40 Hz). In reality, it is possible for an expected 5% of all the values to be above 0.03 if the process were Gaussian. In the above example, the process is harmonic and there is very little power at any other frequencies.

Let us now add a random phase component at the sum frequency of 90 Hz such that there is partial phase coupling rather than perfect phase coupling. The

© 2013 Global Journals Inc. (US)

bicoherence at (50 Hz, 40 Hz) will now be the ratio of the power of the phase coupled component to the total power which is the sum of the powers of the phase coupled and random phase components since these are statistically independent.

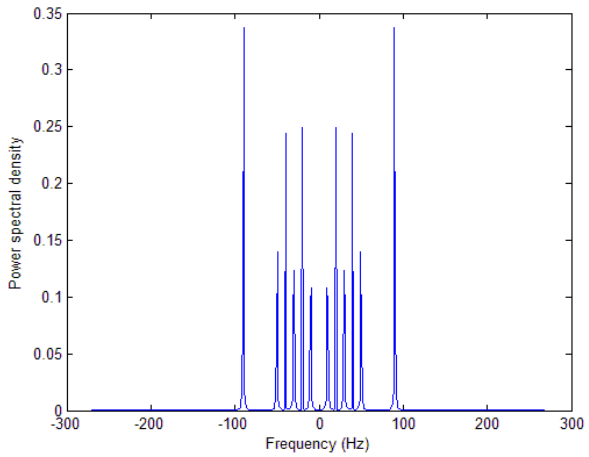

Figure 7 : Power spectral density of the process in equation (21) with an additional random phase component of equal power at 90Hz. The simulations also have additive Gaussian noise and the SNR is 20 dB

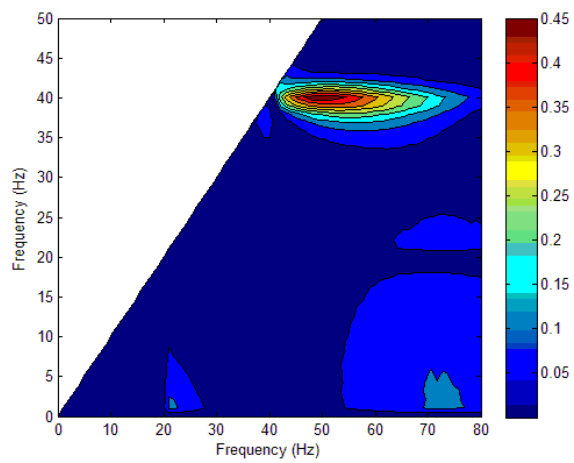

Figure 8 : Bicoherence for the same process as described for figure 7. The bicoherence at (50 Hz, 40 Hz) has now reduced to around 0.5 instead of 1.0 compared to Figure 6

Further, let us add Gaussian noise to the process such that the ratio of the total signal power to the total noise power is 20 dB. If we then compute the power spectrum and the bicoherence, they are as shown in Figure 7 and Figure 8, respectively.

We can see that the estimated bicoherence is close to the expected true value of 0.5. The estimate will in practice have a possibly non-zero bias and finite variance, which depend on a number of factors including the true value and the number of realizations averaged. Analytical expressions for these can be quite complicated. Statistics of bicoherence and tricoherence have been investigated numerically and analytically in [34],[61]. When phase coupled and random phase components are present along with additive Gaussian noise of significant variance, the estimate can be significantly different from the value expected. As the SNR falls, the statistics of the distribution will be decided by the noise rather than by the signal (the phase coupled harmonic components in the example above).

If the hypothesis to be tested is whether the signal is Gaussian or not, we can potentially use bicoherence values from all frequency triads along with the knowledge of their distribution for a Gaussian process. If we simulate 100 records consisting purely of Gaussian random noise of unit variance with the same sampling frequency and record length as in the examples above the bicoherence plot would be as shown in Figure 9 and the histogram of bicoherence values would be as shown in Figure 10. The red line indicates the bicoherence value below which 95% of all bicoherence lie. It can be observed that this is close to 6 divide by twice the number of realizations averaged or 0.03.

As we increase the number of realizations averaged, bicoherence tends towards the expected value of zero for white Gaussian noise.

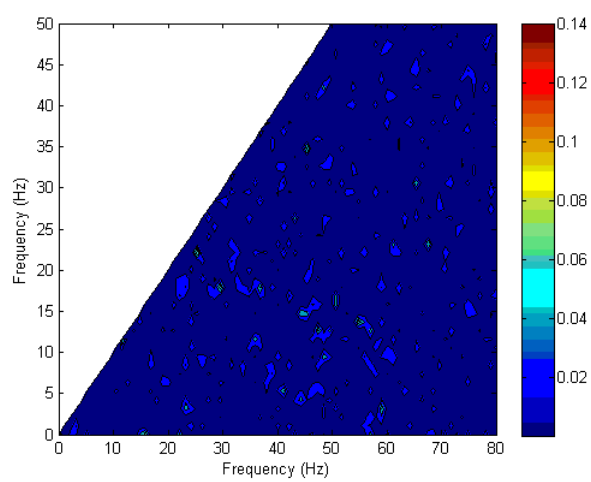

Figure 9 : Bicoherence distribution for a white Gaussian noise process over the same region as shown for the harmonic process in figures 6 and 8 and with the same number of realizations averaged. 5% of the values are now expected to be above the 95% significance level of 0.03 and some of these shows up as the lighter spots

© 2013 Global Journals Inc. (US)

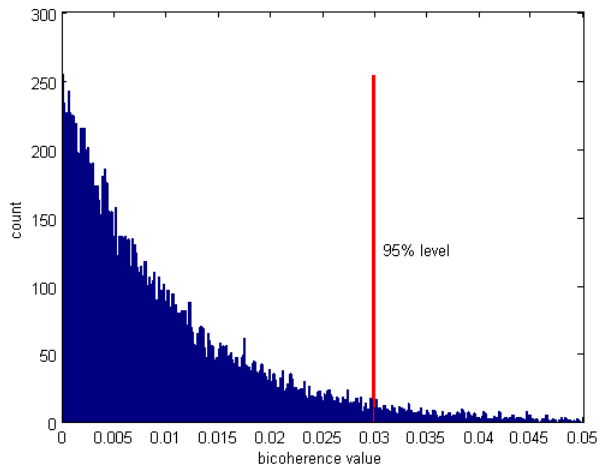

Figure 10 : Bicoherence distribution for a white Gaussian noise process when N=100 realizations are averaged in the estimate. The values are sorted and the value below which 95% lie is determined and shown using the red line above. It can be observed that this value is very nearly equal to 3/N = 0.03

If we want to test the hypothesis that a process is non-Gaussian, we can use this procedure and utilize the distribution of bicoherence over all bi-frequencies or any statistic derived from it. If we want to test whether the bicoherence at a given bi-frequency arose from phase coupled Fourier components or not, we can compare the bicoherence value to the 95% significance level for Gaussian noise. If the value is above this, we can be 95% confident that the true value was not zero. 5% of the values even from Gaussian noise can be above this level. The 99% confidence level is given by 9.2 divided by twice the number of realizations averaged. The higher the bicoherence estimate compared to these and the greater the number of realizations averaged, the greater the confidence in the estimate.

Let us now lower signal to noise power ratio to 40 dB and observe its effect on the power spectrum and the bispectrum. As shown in Figure 11, the power spectrum estimated by an averaged periodogram now shows spurious peaks at many frequencies owing to white noise. The variance at the true signal peaks is also higher. Because the signal is harmonic and comprises of narrowband components, the signal peaks are still above the wideband noise floor.

But the power spectrum does not retain any phase relationships. If we examine the bicoherence, as shown in Figure 12, we can note that the bicoherence at (50Hz, 40 Hz) is significantly above 0.03, the 95% confidence level for Gaussian noise, indicating that it is non-zero.

It is however far from the true value of 0.5 that would be expected from the harmonic components alone. This is owing to a bias introduced by the additive noise which will act as an additional random phase component or components within the bandwidth of the signal.

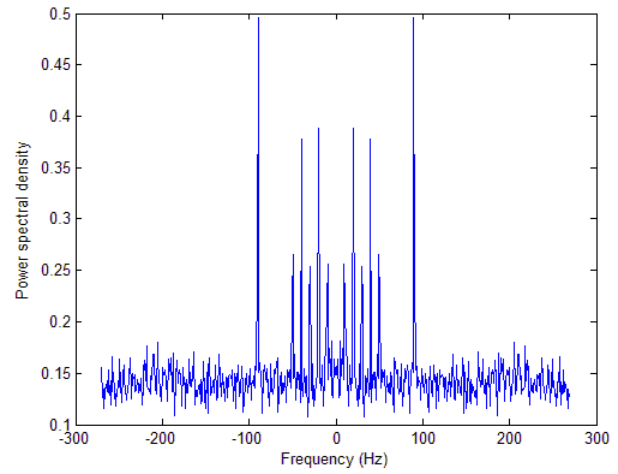

Figure 11 : Power spectral density of the same harmonic process as in figure 7 but with SNR lowered to -40 dB

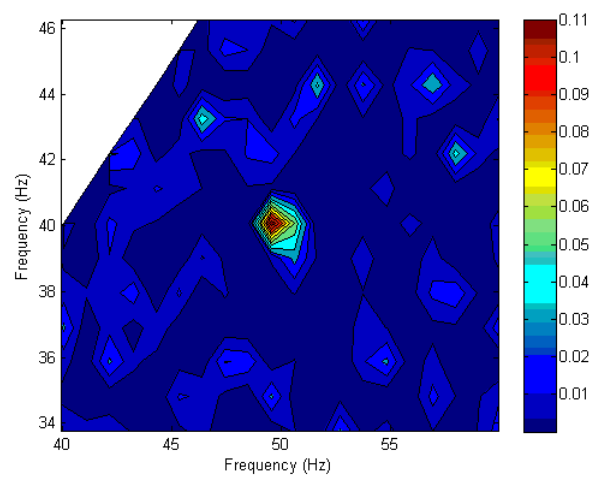

Figure 12 : Bicoherence plot for the same harmonic process as in figures 7 and 8 but with SNR lowered to -40 dB. Some values are above the 95% significance level of 0.03 as can be expected because of the additive white Gaussian noise present. The bicoherence at (50 Hz, 40 Hz) is lowered from 0.5 because of the wideband noise contribution within the signal bandwidth that acts as an additional random phase component

If we increase the number of realizations averaged to 1000, the distribution of bicoherence owing to Gaussian noise alone would tend towards zero, but the bias will depend on the SNR and will not decrease similarly. A bicoherence plot for 1000 realizations averaged is shown in Figure 13 below.

© 2013 Global Journals Inc. (US)

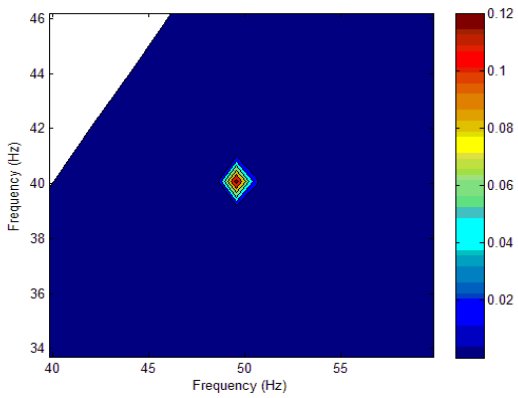

Figure 13 : Bicoherence for the same process as shown in Figure 12, but with 1000 realizations averaged in the estimate instead of 100. The 95% significance level for zero bicoherence is now 0.003. Therefore, the spuriously high bicoherence values appearing in Figure 12 have disappeared. However, the random phase components at 50 Hz, 40 Hz and 90 Hz owing to noise are present in all realizations and the bicoherence at (50 Hz, 40 Hz) remains close to 0.11, a value determined by the power ratio of phase-coupled and random phase components

Note that spurious values of high bicoherence arising at other bi-frequencies have decreased compared to Fig. 12 but the value of bicoherence at (50 Hz, 40 Hz) has not become 0.5.

In spite of a number of limitations, by contrast, the conventional methods for bispectrum estimation can serve as better quantifiers of phase coupling whereas the parametric methods such as autoregressive (AR), moving average (MA) and autoregressive moving average (ARMA) are better as detectors rather than quantifiers [12]. Of course, the conventional bicoherence index approach to serve as a good quantifier by providing good estimates of the degree of phase coupling at harmonically related frequency pairs. For details and excellent explanation of quadratic phase coupling based on conventional and parametric methods, the readers are referred to [4, 12, 13].

Swami *et al* have shown [16] that the trispectrum can be used to resolve cubic phase coupling if a signal contains components from both quadratic and cubic phase coupling. The bispectrum of that signal is blind to the cubically-coupled components and can resolve the quadratically-coupled components, whereas the trispectrum of that signal is blind to the quadratically-coupled components and can resolve the cubically coupled components [11]. Higher-order spectra can thus resolve various types of nonlinearity. An application of higher order spectra to detect quadratic and cubic non-linear characteristics of the output of a non-linear system can be found in the work on analysis of Chua's circuit by Elgar and Chandran [40]. This circuit can exhibit various modes of operation depending on the circuit parameters. It shows periodic outputs, period doubling phenomena and can be in different chaotic regimes. Using bicoherence and tricoherence plots, Elgar and Chandran demonstrate that quadratic interactions are absent when the circuit exhibits the double scroll attractor behavior as evidenced by statistically zero bicoherence. The tricoherence remains significantly non-zero pointing to the presence of cubic phase coupling and interactions. By contrast, when the circuit exhibits Rossler attractor behavior, both the bicoherence and the tricoherence are statistically significantly non-zero and both quadratic and cubic interactions are inferred to be important to the dynamics.

b) Harmonic Retrieval

In several signal processing applications, for instance in estimating the direction of arrival (DOA) of narrow-band source signals with linear arrays and in the harmonic retrieval problem, the estimation of the number of harmonics and the frequencies and amplitudes of harmonics from noisy measurements is frequently encountered. With real signals $x(n)$ for the retrieval of harmonic in noise (RHN) problem, consider the system model is

$$y(n) = \sum_{i=1}^{p} a_i \sin(\omega_i n + \theta_i) + w(n) = x(n) + w(n) \quad (34)$$

where the θ_i's denote random phases which are i.i.d. and uniformly distributed over $(0,2\pi)$, the ω_i's are unknown deterministic frequencies and the a_i's are unknown deterministic amplitudes. The additive noise $w(n)$is assumed to be white or colored Gaussian noise with unknown spectral density. The goal of this problem is to estimate the number of signals *p*, the angular frequenciesω_i's and the amplitudes a_i's.

Second-order statistics based high resolution methods such as MUSIC (Multiple Signal Classification) combined with singular value decomposition work well to estimate the number of harmonics *p* and their parameters if the additive noise is white. However, these methods break down in the case of colored noise to overestimate the number of sinusoids by treating the colored noise as additional sinusoids. Higher-order statistics have been successfully applied to this problem as they show robustness to additive Gaussian noise even when it is coloured.

Third-order cumulants for $y(n)$ equal zero; hence, this is an application where one must use fourth-order cumulants. According to Swami and Mendel [16], the fourth-order cumulants of $y(n)$ is a function of three lags. However, the diagonal slice of this cumulant is given as

$$c_4^y(\tau_1,\tau_2,\tau_3) \triangleq c_4^y(\tau) = -\frac{3}{8}\sum_{i=1}^{p} {a_i}^4 \sin(\omega_i \tau) \quad (35)$$

© 2013 Global Journals Inc. (US)

The autocorrelation of $y(n)$ is given by

$$c_2^y(\tau) = \frac{1}{2}\sum_{i=1}^{p} a_i^2 \, sin\,(\omega_i \tau) \tag{36}$$

Except for a different scale factor, the fourth-order cumulants $c_4^y(\tau)$ from equation (35) and (36) can be easily treated as an autocorrelation function of the following signal which is directly related to $y(n)$:

$$y_1(n) = \sum_{i=1}^{p} a_i^2 \sin(\omega_i n + \theta_i) + w(n) \tag{37}$$

Thus, for the RHN and DOA problem, the diagonal slice of fourth-order cumulant retains all the useful signal characteristics, and consequently, signal parameters can be estimated. Additionally, we show that the 1-D slice is identical with the autocorrelation of a related noiseless signal.

c) Array Processing

One of the most fundamental problems in signal processing is that of removing noise and interference from a received sensor signal. There are two general approaches. Single-sensor methods such as the celebrated Wiener filter enhance the signal by emphasizing frequencies with a high signal- to- noise ratio (SNR) while attenuating those with a low SNR. On the other hand, multichannel techniques employ an array of sensors that perform spatial discrimination or beamforming to aid in removing the unwanted noise. Array processing problems include: directional of arrival (DOA) determination, determination of number of sources, beamforming, estimation of the source signal, source classification, sensor calibration, etc., and the readers refer to [17] for an excellent introduction to array processing and its associated models.

Although many novel and interesting array processing algorithms have appeared, higher-order statistics have been used to solve the array processing problem due to a number of reasons, namely: (1) Capon's minimum-variance distortionless response (MVDR) beamformer, that has been the starting point for both signal enhancement and high-resolution DOA estimation, requires very specific and detailed information about the so-called array steering vector(e.g., source steering angles, array geometry, receiver responses), information that is often not available, or if available is not given to a high degree of accuracy; (2)When additive noise is colored and Gaussian, a second-order statistics based high-resolution DOA algorithm, such as MUSIC, does not perform well, however a cumulant-based MUSIC algorithm does perform well; (3) most second-order statistics based beamformers assume that the received signals are not coherent, which rules out the important case of multipath propagation; cumulant-based beamformers can work in the presence of multipath[18].

Dogan et al used cumulants of received signals to estimate the steering vector of a narrowband non-Gaussian desired signal in the presence of directional Gaussian interferers with unknown covariance structure. They assume no knowledge of the DOA information about the desired signal. The desired signal could be voice speech, sonar and radar return signal.

For radar return signal, consider an array of M elements with arbitrary sensor response characteristics. Assume that the Gaussian interference signal, $i(t)$ with J number and the non-Gaussian desired signal, $d(t)$ at center frequency, f_0. The additive noise is assumed to be Gaussian with unknown covariance. Consequently, the array of M elements measurements can be collected together to give the following model.

$$\boldsymbol{r}(t) = \boldsymbol{a}(\theta_d)d(t) + A_I(\boldsymbol{\theta})\boldsymbol{i}(t) + \boldsymbol{n}(t) \tag{38}$$

where θ_d is the DOA of the desired signal, $\boldsymbol{a}(\theta_d)$ is the array steering vector of the desired signal, $A_I(\boldsymbol{\theta})$ is the array steering matrix for the J interference sources $i(t)$, $\boldsymbol{\theta}$ is a $J \times 1$ vector of DOA's for the interferers, $\boldsymbol{r}(t)$ and $\boldsymbol{n}(t)$ are the $M \times 1$ vector of received signals and Gaussian noises respectively.

The output of an MVDR beamformer can be expressed by Capon [20] as

$$\boldsymbol{y}(t) = \boldsymbol{w}^H\boldsymbol{r}(t) = [\beta_1 R^{-1}\boldsymbol{a}(\theta_d)]^H \tag{39}$$

where constant β_1 is a constant which maintains a specified response for the desired signal, $\boldsymbol{w}$ denotes the weight vector of the processor and R is the covariance matrix of $\boldsymbol{r}(t)$.

Now, by using the properties of cumulants which are described by Mendel [11] and the receiver model in equation (28), Dogan and Mendel show that

$$\boldsymbol{c} = \beta_2\boldsymbol{a}(\theta_d) \tag{40}$$

where β_2 is a another constant. It is said that $\boldsymbol{c}$ is a replica of the steering vector of the desired signal up to a scale factor β_2.

Combining equation (39) and (40), it is shown that the cumulant-based MVDR beamformer output is

$$y(t) = \boldsymbol{w}_{cumulant}{}^H\boldsymbol{r}(t) = [\beta_3 R^{-1}\boldsymbol{c}]^H\boldsymbol{r}(t) \tag{41}$$

where $\beta_3 = (\boldsymbol{c}^H R^{-1}\boldsymbol{c})^{-1}$

At present, HOS has become attractive in array signal processing due to two additional reasons, namely (1) HOS can increase the effective aperture of an array, and (2) HOS can not only eliminate the effects of additive Gaussian noise, but it can also eliminate the effects of additive non-Gaussian noise.

d) Blind Deconvolution and Equilazation

The blind deconvolution or equalization problem, deals with the reconstruction of the input sequence given the output of a linear system and statistical information about the input. Blind

© 2013 Global Journals Inc. (US)

deconvolution algorithms are essentially adaptive filtering algorithms [17] designed in such a way that do not need the external supply of a desired response to generate the error signal in the output of the adaptive equalization filter whereas Classical deconvolution is concerned with the task of recovering an excitation signal, given the response of a known time-invariant linear operator to that excitation [19]. Blind deconvolution algorithm itself generates an estimate of the desired response by applying a non-linear transformation on sequences involved in the adaptation process. Detailed discussion on blind deconvolution can be found in [5].

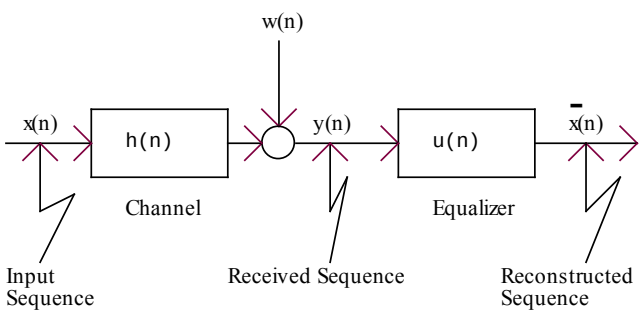

Figure 14 : Block diagram of a baseband communication system subject to additive noise

Let us consider a discrete-time linear transmission channel with impulse response, $h(n)$ which is unknown and time-varying. The input signal $x(n)$ is assumed to be independent and identically distributed (i.i.d) random variables with a non-Gaussian probability density function, with zero mean and variance. Initially the noise will not be taken into account in the output of the channel which can be written as from Figure 14.

$$y(n) = h(n) * x(n) = \sum_{i=-\infty}^{+\infty} x(n)h(n-i) = \sum_{i=-\infty}^{+\infty} h(n)x(n-i) \quad (42)$$

Table 1 : Summary of Developed Blind Equalization Algorithm Based on Higher-order Statistics

Develop algorithm	Significant work	Related Reference
Tricepstrum Equalization Algorithm (TEA)	Estimate the equalizer impulse response by using the complex cepstrum of the fourth-order cumulants of the synchronously sampled received signal.	[Hatzinako and Nikias,1991]
Power Cepstrum and Tricoherence Equalization Algorithm (POTEA)	Recovers the Fourier magnitude of the equalizer using autocorrelations and its Fourier phase fourth-order cumulants and the cepstrum of the Tricoherence.	[Bessios and Nikias, 1991]
Cross-Trispectrum Equalization Algorithm (CTEA)	Extension of TEA to the multichannel case using the cross-cumulants of the observed signals.	[Brooks and Nikias, 1991]

The goal of this problem is to restore $x(n)$ from the received sequence $y(n)$ to identify the inverse filter, $u(n)$ of the channel.

From Figure 14, it is seen that the reconstructed signal $\tilde{x}(n)$ of the equalizer is given by

$$\tilde{x}(n) = u(n) * y(n) = u(n) * h(n) * x(n) \quad (43)$$

It is achieved that the output reconstructed signal $\tilde{x}(n)$ is given by

$$\tilde{x}(n) = x(n-D)e^{j\theta} \quad (44)$$

where D and θ are a constant delay and a constant phase shift respectively. The convolution sum of the equalizer function and channel response function can be written as

$$u(n) * h(n) = \delta(n-D)e^{j\theta} \quad (45)$$

where $\delta(n)$ is the Kronecker delta function. Taking the Fourier transform of equation (45) and we obtain

$$U(\omega)H(\omega) = e^{j(\theta-\omega D)} \quad (46)$$

Hence, the objective of the equalizer is to achieve a transfer function

$$U(\omega) = \frac{1}{H(\omega)} e^{j(\theta-\omega D)} \quad (47)$$

In general, D and θ are unknown. However, the constant delay D does not affect the reconstructed of the original input signal, $x(n)$. The phase constant, θ can be removed by a decision device.

Blind equalization algorithms based on higher-order statistics (HOS) perform a nonlinear transformation on the input of the equalizer filter. This nonlinear transformation is memory nonlinearity and it is identical to the generation of higher-order cumulants of the received channel data. For more details, the readers are referred to the following table 1, about the various algorithms of blind equalization based higher-order statistics.

© 2013 Global Journals Inc. (US)

e) Narrow and Wide band Interference Cancellation

When a modulating signal is corrupted by an additive interference and an auxiliary reference signal which is highly correlated with the interference, the elimination of the interference is accomplished by an adaptive noise canceller using fourth-order statistics procedure which is shown in Fig. 4. The objective of an adaptive noise canceller is to produce a system output that best fits with the modulating signal. A conventional ANC which is called adaptive noise canceller second-order statistics (ANC-SOS) algorithm cannot be applied in practice due to two major difficulties, namely (1) the ANC-SOS filter is affected directly by uncorrelated noises at the primary and reference inputs, (2) the ANC-SOS algorithm is problem dependent, i.e., it is very sensitive to both the reference signal statistics and the choice of step size.

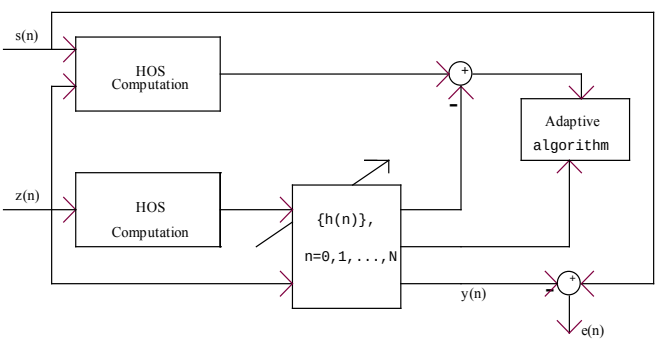

Figure 15 : Block diagram of adaptive interference canceller based on higher-order statistics

Let $x(n)$ and $z(n)$ denote the received signal and interference signal sequence respectively, they are both sampled in chip rate, satisfying

$$x(n) = s(n) + i(n) + n_p(n) \tag{48}$$

$$z(n) = w(n) + n_r(n) \tag{49}$$

where $s(n)$ is the modulating signal, $i(n)$ is the narrowband interference signal, and $w(n)$ is a zero-mean non-Gaussian reference signal highly correlated with the interference. The measurement noise $n_p(n)$ and $n_r(n)$ are stationary, zero-mean, white or colored Gaussian process. The interference can be described by the interference signal as

$$i(n) = \sum_{k=-\infty}^{+\infty} g(k)w(n-k) \tag{50}$$

Let $y(n)$ be an adaptive filter output

$$y(n) = \sum_{k=0}^{N-1} h(k)z(n-k) \tag{51}$$

where N denotes the number of taps and $\{h(n), n = 0,1,\dots,N-1\}$ is the adaptive filter coefficients. The system output $e(n)$ is an evaluate of modulating signal $s(n)$, which is given by

$$e(n) = x(n) - y(n) \tag{52}$$

f) Time-Delay Estimation

Time-delay estimation is one of most important method for broad-band source bearing and range calculation.

Assume that $x(n)$ and $y(n)$ are two discrete time signals which are spatially separated sensor measurements that satisfy the following equations

$$x(n) = s(n) + w_1(n) \tag{53}$$

$$y(n) = As(n-D) + w_2(n) \tag{54}$$

where $s(n)$ is an unknown broad-band source bearing signal, $s(n-D)$ is D unit delay version of $s(n)$ and $w_1(n)$ and $w_2(n)$ are unknown noise source. The basic approach to solve the time delay estimation problem is to shift measurement sequence $x(n)$ with respect to $y(n)$ by taking cross correlation technique and we obtain.

$$\begin{aligned} c_{xy}(\tau) &= E\{x(n)y(n+\tau)\} = E\{x(n+\tau)y(n)\} \\ &= \sum_{n=-\infty}^{+\infty} x(n)y(n+\tau) = \sum_{n=-\infty}^{+\infty} x(n+\tau)y(n) \\ &= Ac_2^s(\tau - D), \qquad -\infty < \tau < +\infty \end{aligned} \tag{55}$$

Equation (53) and (54) provided that $w_1(n)$ and $w_2(n)$ are zero-mean stationary signals which are independent with each other with $s(n)$ and $c_2^s(\tau) = E\{s(n)s(n+\tau)\}$ is the covariance sequence of $s(n)$. In practical situations, due to finite length data records and noise source that are not exactly independent, the $c_{xy}(\tau)$ does not necessary to show peak at $\tau = D$ at time delay D. It is well known to [21], Carter said that various window technique such as ROTH, SCOT, PHAT, Eckart and Hannan-Thompson have been suggested to smooth the cross-correlation function in order to improve the quality of time delay estimation.

g) Classification

Signal classification can be done working directly with the signal samples, or with the attributes related to them. It is difficult to handle additive colored Gaussian noise with traditional approaches. A new approach [22] that is blind to additive colored or white Gaussian noise, works with vector of cumulants or higher order spectra, and extends correlation-based classification to HOS-based classification. It is based on the important fact that estimates of cumulants or higher order spectra are asymptotically Gaussian. Consequently, one is able to begin with an equation like 'Estimate of HOS = HOS + estimation error' In which the "estimation error" is asymptotically Gaussian and extend traditional classification or detection procedures

© 2013 Global Journals Inc. (US)

to this information. Working with a vector of higher-order statistics is in the spirit of using attributes which are derived from the original data. Consequently, higher-order statistics now provide new attributes to be used in signal classification problems including detection.

By minimizing a distance measure in the cumulant domain Tsatsanis et al built shift-invariant and noise-insensitive classifiers which are summarize in table 2. For more details, the readers are referred to [23]

IV. Application to Communication Systems

Wireless single input- single output (SISO) techniques like BPSK, OQPSK, MSK, GMSK are used commonly in modern communication [24]. Most communication signals are corrupted by noise, thus it seems particularly important to detect signals more effectively at low SNR. There are many algorithms of signal detection and recognition based on higher-order statistics now, but few at low SNR. Furthermore, there are fewer algorithms based on higher-order statistics at low SNR with non-Gaussian background.

The bi-spectrum has been used in a technique [24] to suppress Gaussian noise for increasing the channel capacity (bit/s) as well as to test the inhibition effect of higher order statistics and the detection effect of BPSK, OQPSK, MSK, GMSK signals based on bi-spectrum in different SNR. Using the third order cumulant, Zhong Zhang et all used Matlab software [24] for finding the detection rate, by assuming following parameters:

Table 2 : Summary of Object CLASSIFYING BASED on Higher-Order Statistics

Classification	Block diagram	Algorithm's procedure
Shift-invariant Classification	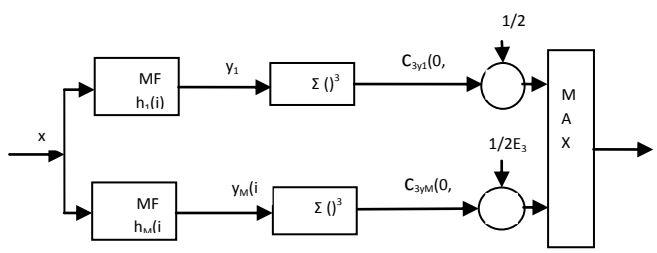	Step 1. Build a bank of filters $\{h_m(i)\}_{i=0}^{N}$, where each one is matched to a template $h_m(i)= s_m(N-i)$, $m=1,\dots,M$. Step 2. Filter $x(i)$ through these filters and compute $y_{3m}(0,0)$ at the output of each filter. Step 3. Add the bias term $\frac{1}{2}E_{3m}$ at the output of each matched filter to compensate for templates with unequal triple correlation energies. Step 4. Select the maximum, say m^*, to declare H_m .
Rotation- and Scaling- invariant Classification	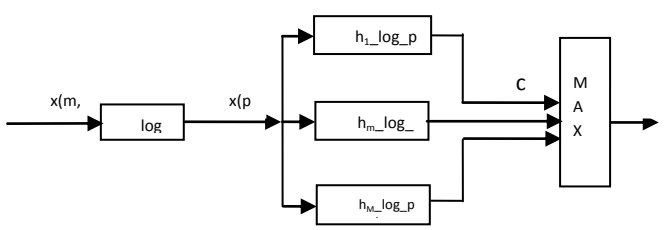	Step 1. Transform all templates to log-polar grid and design a bank of filters matched to the transformed templates. Step 2. Transform the input image to log-polar grid. Step 3. Apply the translation invariant algorithm to the transformed image.
Shift, Rotation and Scaling-invariant Classification	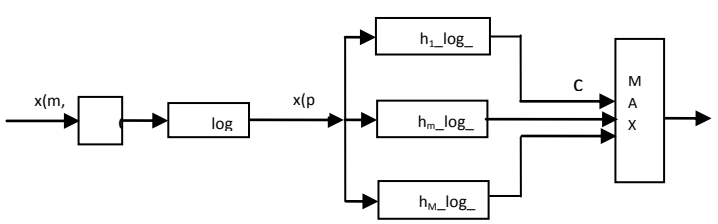	Step 1. Compute the zeroth slice $x_3(i_1,0)$ of the triple correlation of x_i. Step 2. Sample it in a log-polar grid to form $x_3[(\log\rho,\theta);0]$. Step 3. Apply the rotation-scaling invariant algorithm to $x_3[(\log\rho,\theta);0]$.

© 2013 Global Journals Inc. (US)

Table 3 : Bi-Sectrum Processing Effect of BPSK, OQPSK, MSK, GMSK Signal at Different SNR

Communication Signal Processing	SNR in dB	Detection Rate
BPSK (Binary Phase Shift Keying)	0	100%
	-4	100%
	-8	100%
	-12	95%
	-14	65%
OQPSK (Orthogonal Quadratic Phase Shift Keying)	0	100%
	-4	100%
	-8	100%
	-12	80%
	-14	60%
MSK (Minimum Phase Shift Keying)	0	100%
	-4	100%
	-8	100%
	-12	75%
	-14	60%
GMSK (Gaussian Minimum Shift Keying)	0	100%
	-4	100%
	-8	100%
	-12	70%
	-14	65%

Sample points: 3840, Carrier frequency: 150000 Hz, Sampling frequency: 1200000Hz, Code rate: 125000, SNR: -14db, which is shown in table 3.

On the other hand, table 3. shows that the detection rate decreases with SNR decreased. On the other hand, four signals can achieve the desired detection effect at 0,-4,-8 db and detection rate starts to decline from -12db. According to the different signals and different intensity of background noise, an effective detection rate can be obtained using higher-order cumulant.

Li Taijie et al proposed a Genetic algorithm which is independent of both noise source and reference signal as well as HOS which can preserve information of non-Gaussian stationary random process [25].Compare with the adaptive filters based on second-order statistics, the HOS and GA-based filter can reject the interference more efficiently and is independent of uncorrelated Gaussian noise. So it is important to obtain an algorithm which is independent of both uncorrelated noise sources and the statistics of the reference signal. For this purpose, D.C. Shin and C.L. Nikias [26] have introduced an adaptive scheme based on HOS for narrow band interference rejection.

Besides, Spread spectrum is itself a powerful technique to mitigate multipath propagation but when, as in Cellular CDMA (Code Division Multiple Access), bandwidth limitations are consequent to system design considerations, other counter measures must be adopted [30], 31], [33]. Multipath propagation degrades system performance not only because it introduces intersymbol interference (ISI) but also because it deteriorates the orthogonality property of the spreading codes. To overcome this limitation, Massimiliano Martone [27] studied a cellular direct sequence spread spectrum CDMA system which seems to be attractive due to numerical stability and computational complexity based on fourth order cumulants with respect to TDMA and FDMA.

In many applications, it is desired to extract some information from a signal corrupted by multiplicative noise. One such application lies in mobile communications where the transmitted signals are bandlimited, frequency or phase-modulated signals, $T_x(t)$ is given by

$$T_x(t) = Ae^{j\left(2\pi f_0 t + \phi(t)\right)} \tag{56}$$

where $\phi(t)$ represents the baseband signal, f_0 is the carrier frequency and A is the constant amplitude of the transmitted signal. The mobile radio channel is a time-varying multipath channel and is subject to physical propagation path loss [28].The time-variations are caused by the medium changes as the vehicles moves. The propagation losses are related to both the atmospheric propagation and the terrain configuration. The multipath aspect is caused by different scatterers and reflectors such as buildings or trees that surround the mobile unit which is shown in Figure 16.

As a result of these propagation phenomena in a narrow-band transmission, where narrow-band is defined with respect to the coherence bandwidth of the channel [22], the received signal $R_x(t)$ is given by:

$$R_x(t) = Ae(t)e^{j\left(2\pi f_0 t + \phi(t) + \psi_r(t)\right)} \tag{57}$$

where $e(t)$ and $\psi_r(t)$ are respectively a Rayleigh distributed random amplitude modulation signal and a uniformly distributed random phase.

Both $e(t)$ and $\psi_r(t)$ affect the performance of the receiver which results in an increase of bit-error rate. Current techniques for reducing the effect of the Rayleigh multiplicative noise are based on the use of diversity techniques,[28]. As a matter of fact, a new cost-effective method based on Time-varying Higher Order Spectra (TV-HOS), particularly the Wigner-Ville Trispectrum (WVT) is proposed for optimal recovery of the information contained in the signal without use of diversity techniques in [29].

© 2013 Global Journals Inc. (US)

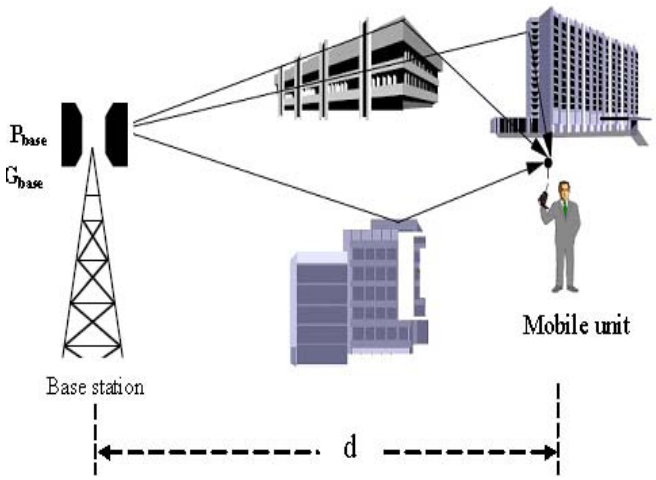

Figure 16 : Multipath Fading Phenomenon

For non-stationary random signal, Time-Varying Higher-Order Spectra (TV-HOS) extends the class of Polynomial Wigner-Ville Distributions (PWVD). The k-th order Wigner-Ville spectrum of a random signal $x(t)$ is defined as

$$\mathrm{M}_x^k(t,f) = \int_{-\infty}^{+\infty} m_x^k(t,\tau)\, e^{-j2\pi f\tau}\, d\tau \qquad (58)$$

where $m_x^k(t,\tau)$ represents a specific slice of the time-varying k-th order moment function of $x(t)$ and is expressed as

$$m_x^k(t,\tau) = E\left(x^*(t+\lambda_1\tau)\prod_{i=1}^{k-1} P_{i+1}\left[x(t+\lambda_{i+1}\tau)\right]\right) \qquad (59)$$

where $(\lambda_1,\dots,\lambda_k)$ determines the slice, * represents the complex-conjugate operator, $P_{i+1}[.]$ is the complex conjugate operator and identity operator if i is odd and even respectively, and $E(.)$ is expectation function.

For $k=4$, the k-th order Wigner-Ville spectrum converts to Wigner-Ville Trispectrum which is defined as

$$\begin{aligned} M_x^4(t,f) &= E\left(W_x^4(t,f)\right) \\ &= \int_{-\infty}^{+\infty} E\left[x\left(t+{}^{\tau}/_{4}\right)^2 x^*\left(t-{}^{\tau}/_{4}\right)^2\right] e^{j2\pi f\tau}\, d\tau \end{aligned} \qquad (60)$$

where $W_x^4(t,f)$ is the fourth-order Polynomial Wigner-Ville Distribution (PWVD) function of $x(t)$and $M_x^4(t,f)$ is referred to as moment-based Wigner-Ville Trispectrum (WVT).

In [29] this moment based WVT which is described in equation (48), in particular, is successful to recover the spectral characteristics as well as optimum estimation of the instantaneous frequency (IF) of the signals for increasing the system performance.

V. Potential of HOS for Further Applications

SISO systems are used commonly in modern communication system owing to their reduced cost and complexity. But most communication signals encounter degradations in channel (e. g. scatters and reflectors such as buildings and trees) and it is particularly important to detect signals effectively at low SNR.

MIMO systems show promise in this context. It may be possible to use HOS to analyze MIMO system performance taking mutual electromagnetic coupling of antenna elements into consideration.

Non-stationary and cyclostationary signal analysis with HOS-based time frequency representations can reveal information on sub-manifolds in higher dimensional frequency spaces that offer greater SNR pathways in available channels. It can lead to design of coding techniques that may be superior to those based on second order information theory concepts and channel capacity limits.

VI. Conclusion

Regardless of the use of diversity or spatial multiplexing technique, the main drawback of any MIMO system is increased complexity and cost. Due to this reason, there is now great interest in Higher Order Spectra based schemes. HOS can be applied in transmitter section, receiver section or on both sides and have the potential to retain the performance improvement similar to that of a full complexity MIMO system at reduced complexity and cost. In addition, spectrum estimation techniques have proved essential to the creation of advanced communication systems. These techniques only use second-order statistical information, which means that we have been assuming that the signals are inherently Gaussian. Most real – world signals are non Gaussian. It is no wonder, therefore, that spectral techniques often have serious difficulties in practice. For this reason, there is a need for a thorough literature review and original innovations in this area with emphasis on wireless communication and pattern recognition and so on.

There is much more information in a stochastic non-Gaussian or deterministic signal than conveyed by its auto- correlation or spectrum. Higher-order spectra, which are defined in terms of the higher-order statistics of a signal, contain this additional information.

Signal processing algorithms based on higher-order spectra are now available for use in commercial and military applications. The emergence of low cost very high speed hardware chips and the ever growing availability of fast computers now demand that we extract more information than we have been doing in the past from signals, so that better decisions can be made. All of the new algorithms that have been developed

© 2013 Global Journals Inc. (US)

using higher-order spectra are application driven. That is why higher order spectra (HOS) are an attractive scheme for the above mentioned field.

Acknowledgement

The material presented in this paper is based on the textbook by C.L Nikias and A.P. Petropulo, Higher- Order spectral Analysis, Oppenheim Series of Signal Processing, Prentice-Hall, Inc. 1993 as well as the tutorials by C.L. Nikias and M.R. Raghuveer, “Bispectrum Estimation: A Digital Processing Framework”, Proc. IEEE, Vol. 75, july 1987.

References Références Referencias

1. D. R. Brillinger and M. Rosenblatt, "Asymptotic theory of estimates of k-th order spectra," in *Spectral Analysis of Time Series,* B. Harris, Ed. New York: Wiley, 1967a, pp. 153-188.
2. D. R. Brillinger and M. Rosenblatt, "Computation and Interpretation of k-th order spectra," in *Spectral Analysis of Time Series,* B. Harris, Ed. New York: Wiley, 1967b, pp. 189-232.
3. K. Hasselman, W. Munk, and G. MacDonald, "Bispectra of ocean waves," in *Time Series Analysis,* M. Rosenblatt, Ed. New York: Wiley, 1963, pp. 125-130.
4. C. L. Nikias and M. R. Raghuveer, "Bispectrum Estimation – A Digital Signal Processing Framework," *Proc. Of the IEEE,* vol. 75, pp. 869-891, 1987.
5. C. L. Nikias and A. Petropulu, *Higher–order spectra analysis: A nonlinear signal processing framework*. Englewood Cliffs, NJ: Prentice Hall, 1993.
6. B. Boashash, E. J. Powers, and A. M. Zoubir, "Higher-Order Statistical Signal Processing," Melbourne: Longman Australia, 1995.
7. A. N. Shiryaev, " Some problems in the spectral theory of higher order moments," *Theory Prob. Appl.,* vol. 5, pp. 265-284, 1960.
8. D. R. Brillinger, "An Introduction to Polyspectra," *Ann. Math. Statist.,* vol. 36, pp. 1351-1374, 1965.
9. Chandran and S. Elgar, "A general procedure for the computation of principal domains of higher order spectra," *IEEE Trans. On Signal Processing,* vol. 42, pp. 229-233, 1994.
10. W. A. Gardner, *Introduction to Random Processes*. New York: MacMillan, 1986.
11. J. M. Mendel, "Tutorial on higher-order statistics (spectra) in signal processing and system theory: theoretical results and some applications," *Proceedings of the IEEE,* vol. 79, pp. 278-305, 1991.
12. M. R. Raghuveer and C. L. Nikias, "Bispectrum Estimation: A Parametric Approach", *IEEE Transaction on Acoustics, Speech and Signal Processing,* vol. assp-33, no. 4, 1985.
13. Young C. Kim and Edward J. Powers, "Digital Bispectral analysis and its applications to nonlinear wave interactions", *IEEE Transactions on Plasma Science,* vol. ps-7, no. 2, 1979.
14. T. S. Rao and M. M. Gabr, "An introduction to bispectral analysis and bilinear time series models" Lecture notes in Statistics, 24 Springer-Verlag, New York, NY, 1984.
15. D. R. Brillinger, "The identification of a particular nonlinear time series system", Biometrika, vol. 64, no. 3, pp. 509-515, 1977.
16. A.Swami and J. M. Mendel, "Cumulant-based approach to the harmonic retrieval and related problems", *IEEE Transactions on Signal Processing,* vol. 39, pp. 1099-1109, 1991.
17. B.D. Van Veen and K.M. Buckley, "A Versatile approach to Spatial Filtering", *IEEE ASSP Magazine,* pp. 4-24,1988.
18. M.C. Dogan and J.M. Mendel, "Cumulant-based optimum beamforming", USC-SIPI Report # 195, January 1992.
19. J. A. Cadzow, "Blind Deconvolution via cumulant extrema", *IEEE Signal Processing Magazine,* pp. 24-42, 1996.
20. J. Capon, "High-Resolution Frequency-wave number spectral analysis", *Proc. of the IEEE*, vol. 57, no. 8, pp. 1408-1418, 1969.
21. C. L. Nikias and J. M. Mendel, "Signal processing with higher-order spectra", IEEE Signal Processing Magazine, vol. 10, pp. 10-37, 1993.
22. G. B. Giannakis and M. K. Tsatsanis, "Signal detection and classification using matched filtering and higher-order statistics", IEEE transactions on Acoustics, Speech and Signal processing, vol. 38, pp. 1284-1296, 1990.
23. M. K. Tsatsanis and G. B. Giannakis, "Object and Texture classification using higher-order statistics", IEEE Transactions on pattern analysis and machine intelligence, vol. 14, no. 7, 1992.
24. Z. Zhang, W. Yang and Q. Ding, "Communication Signal processing at low SNR using higher-order spectrum", Fourth International Conference on Natural Computation, vol. 1, pp. 65-69, 18-20 Oct. 2008.
25. L. Taijie, H. Guangrui and G. Qing, "Interference rejection in Direct-sequence Spread Spectrum Communication system based on Higher-order Statistics and Genetic algorithm", Fifth International Conference on Signal Processing Proceedings, vol. 3, pp.1782-1785, 2000.
26. D. C Shin and C.L Nikias, "Adaptive Interference canceler for Narrowband and Wideband interference using higher-order statistics", *IEEE transactions on Signal Processing,* vol. 42, no. 10, pp. 2715-2728, 1994.
27. M. Martone, "Blind multichannel deconvolution in multiple access spread spectrum communications

© 2013 Global Journals Inc. (US)

using higher-order statistics", *IEEE international Conference on Communications,* vol. 1, pp. 49-53, 18-22 June 1995.
28. W. Jakes, "Microwave Mobile Communication", John Wiley and Sons, 1974.
29. B. Senadji and B. Boashash, "A mobile communications application of time-varying higher-order spectra to FM signals affected by multiplicative noise", International Conference on Information, Communications and Signal Processing, vol. 3, pp. 1489-1492, 9-12 Sep, 1997.
30. B. Vucetic and J. Yuan, "Space Time Coding", John Wiley and Sons, 2003.
31. D. Tse, P. Viswanath, "Fundamental of wireless communication", Cambridge University Press, 2005.
32. W. H. Tranter, K. S. Shanmugan, T. S. Rappaport and K. L. Kosber, "Principles of Communication systems Simulation with wireless applications", Prentice Hall, 2003.
33. L. C. Godara, "Handbook of antennas in Wireless communication", 888 CRC Press, 2002.
34. Chandran., S. Elgar and B. Vanhoff, Statistics of tricoherence. Signal Processing, IEEE Transactions on, 1994. **42**(12): p. 3430-3440
35. Chandran. and S.L. Elgar, Pattern Recognition Using Invariants Defined From Higher Order Spectra- One Dimensional Inputs. Signal Processing, IEEE Trans. on, 1993. **41**(1): p. 205.
36. V. Chandran. and S.L. Elgar, Mean and variance of estimates of the bispectrum of a harmonic random process-an analysis including leakage effects. Signal Processing, IEEE Transactions on, 1991. **39**(12): p. 2640-2651.
37. V. Chandran. and S.L. Elgar. Position, rotation, and scale invariant recognition of images using higher-order spectra in IEEE International Conference on Acoustics, Speech, and Signal Processing (ICASSP-92), vol. 5, pp. 213-216, 1992
38. V. Chandran. and S. Elgar. Shape discrimination using invariants defined from higher-order spectra in IEEE International Conference on Acoustics, Speech, and Signal Processing (ICASSP-91), vol. 5, pp. 3105-3108, 1991
39. V. Chandran. and S. Elgar. Shape discrimination using invariants defined from higher-order spectra in IEEE International Conference on Acoustics, Speech, and Signal Processing (ICASSP-91), vol. 5, pp. 3105-3108, 1991
40. Elgar, S. and V. Chandran, Higher order spectral analysis of Chua's circuit. Circuits and Systems I: Fundamental Theory and Applications, IEEE Trans. on, 1993. **40**(10): p. 689-692
41. Elgar, S. and V. Chandran, Higher-Order Spectral Analysis To Detect Nonlinear Interactions in Measured Time Series and an Application to Chua's Circuit. International Journal of Bifurcation and Chaos, 1993. **3**(1): p. 19-34
42. Tieu, L., C. Reilly, V. Chandran and S. Sridharan. Postcode segmentation and recognition using projections and bispectral features in Proceedings of IEEE Region 10 Annual Conference on Speech and Image Technologies for Computing and Telecomm (TENCON '97), vol. 1, pp. 47-50, 1997
43. V. Chandran., S. Slomka, M. Gollogly and S. Elgar. Digit recognition using trispectral features in IEEE International Conference on Acoustics, Speech, and Signal Processing (ICASSP-97), vol. 4, 3065-3068, 1997
44. V. Chandran. On the computation and interpretation of auto- and cross-trispectra in IEEE International Conference on Acoustics, Speech, and Signal Processing (ICASSP-94), vol. IV, pp. 445-448, 1994
45. V. Chandran. and S. Elgar. Shape discrimination using invariants defined from higher-order spectra in IEEE International Conference on Acoustics, Speech, and Signal Processing (ICASSP-91), vol. 5, pp. 3105-3108, 1991
46. Ning, D. and V. Chandran, The Effectiveness of Higher Order Spectral Phase Features in Speaker Identification in Odyssey 2004 – The Speaker and Language Recognition Workshop, Toledo, Spain, pp. 245-250, 2004
47. V. Chandran., D. Ning and S. Sridharan, Speaker Identification Using Higher Order Spectral Phase Features and their Effectiveness vis-à-vis Mel-Cepstral Features, in International Conference on Biometric Authentication (ICBA), Hong Kong, China, pp. 614-622, 2004
48. Ong, H. and V. Chandran, Recognition of viruses by electron microscopy using higher order spectral features, in International Society for Optical Engineering (SPIE) - Medical Imaging, San Diego, USA, pp. 234-242, 2003
49. V. Chandran. and S. Elgar, Detection of Sea-mines in Sonar imagery using higher order spectral features, in Proc. of SPIE AeroSense'99, Orlando, Florida, USA, pp. 578-587, 1999
50. Phythian, M., S. Sridharan and V. Chandran, Bispectrum based Cepstral Coefficients for Robust Speaker Recognition in Proc. of Intelligent Signal Processing and Communication Systems (ISPACS'98), Melbourne, Australia, pp. 845-848, 1998
51. Chua, C.K., V. Chandran, R. Acharya and C. Lim, "A review of higher order spectra in biomedical signal processing," Medical Engineering and Physics, vol. 32, page 679-689, 2010
52. B. Chen and V. Chandran, "Biometric Template Security using Higher Order Spectra," Proc. of ICASSP-2010, Dallas, USA, 2010

© 2013 Global Journals Inc. (US)

53. B. Chen and V. Chandran, "Robust Image Hashing using Higher Order Spectral Features," Proc. of DICTA-2010, Sydney, Australia, 2010
54. Chua, C.K., V. Chandran, U.R. Acharya and C.M. Lim, Automatic identification of epileptic electroencephalography signals using higher-order spectra. Proc. Inst. of Mech. Engineers, vol. 223: Part H: Journal of Engineering in Medicine, pp. 485-495, 2009
55. Chua, C.K., V. Chandran, U. R. Acharya and C. M. Lim, "Analysis of epileptic EEG signals using higher order spectra," Journal of Medical & Engineering Technology, UK, 33(1), 2009, 42-50
56. Chua, C.K., V. Chandran, R. Acharya and C. Lim, Cardiac state diagnosis using higher order spectra of heart rate variability Journal of Medical Engineering and Technology, 2007. **32**(2): p. 145 – 155
57. Strange, A.D., J.C. Ralston and V. Chandran, Near Surface Interface Detection for Coal Mining Applications using Bispectral Features and GPR subsurface Sensing Technologies and Applications (SST&A), 2005. **6**(2): p. 125-149
58. Ong, H. and V. Chandran, Identification of gastroenteric viruses by electron microscopy using higher order spectral features. Journal of Clinical Virology, 2005. **34**(3): p. 195-206
59. V. Chandran., S. Elgar and A. Nguyen, Detection of mines in acoustic images using higher order spectral features. Oceanic Engineering, IEEE Journal of, 2002. **27**(3): p. 610-618
60. Elgar, S., B. Vanhoff, L.A. Aguirre, U.S. Freitas and V. Chandran, Higher-order Spectra of Nonlinear Polynomial Models for Chua's circuit International Journal of Bifurcation and Chaos, 1998. **8**(12): p. 2425-2431
61. S. Elgar and R.T. Guza, "Statistics of Bicoherence," IEEE Trans. ASSP, vol. 36, pp. 1667-1668, 1988.

© 2013 Global Journals Inc. (US)